

Estimation of Interpretable eQTL Effect Sizes Using a Log of Linear Model

John Palowitch*, Andrey Shabalin[†], Yihui Zhou[‡]
Andrew B. Nobel*, Fred A. Wright^{‡§}

July 16, 2022

Abstract

Expression Quantitative Trait Loci (eQTL) detection is the task of identifying regulatory relationships between genes and genomic loci. Often, this is performed through a multiple testing procedure, where individual tests are based on regression p-values for gene-SNP pairs. Due to the non-Normality of residuals when raw gene expression data is used, normalizing transformations are usually applied to gene expression as a technique for controlling false discoveries. In this paper, however, we show that the most common transformations are uninterpretable in terms of biological eQTL action, or statistically unjustified with respect to real data. We propose a new model called ACME which respects biological understanding of eQTLs and is corroborated by a real data set provided by the Genotype Tissue Expression (GTEx) consortium. We derive a non-linear least-squares algorithm to fit the model and compute p-values. We argue that the use of the ACME model facilitates accurate and interpretable effect size estimation and p-value computation for the individual gene-SNP pairs relevant to current eQTL studies, and provide careful simulation analyses to ensure that Type-I error is controlled in the absence of the harsher normalizing transformations that ACME avoids. Finally, we provide some basic exploratory downstream analyses incorporating ACME-estimated effect sizes to show the model's potential.

Emails for correspondence: palojj@email.unc.edu, nobel@email.unc.edu, fred_wright@ncsu.edu

*Statistics and Operations Research, University of North Carolina at Chapel Hill

[†]Center for Biomarker Research and Personalized Medicine, Virginia Commonwealth University

[‡]Bioinformatics Research Center and Departments of Biological Sciences, North Carolina State University

[§]Department of Statistics, North Carolina State University

1 Introduction

The discovery of expression Quantitative Trait Loci (eQTL) have become increasingly important as a way to understand the molecular mechanisms by which genetic variation gives rise to complex traits and human disease (14, 8, 9, 22). In particular, eQTL studies have been able to connect Genome-Wide Association Studies (GWAS) to gene expression in ways that acknowledge tissue variation, yielding increased power and insight over GWAS alone (7, 1). Mainly, eQTL studies focus on patterns of associations between single-nucleotide genotypes and gene expression levels, across many genomic loci and transcription sites. Methods to detect and map these associations has given insight into a wide variety of problems, particularly in linking eQTL action to other phenotypes (23). A wide array of statistical methods is now available for these efforts, ranging from standard linear regression (18) to hierarchical Bayesian methods (6). However, these past efforts have focused almost exclusively on detecting eQTL associations without characterizing them. In this paper, our focus is on potential statistical models for the effect size of an eQTL.

Estimated effect sizes of eQTLs are of interest both as a way to rank eQTLs by strength (and, presumably, importance), and as a way to understand the fundamental mechanism of eQTL action. Existing approaches have defined eQTL effect size as the correlation between genotype and expression, measured by the R^2 statistic derived from the model at hand (see for example (19)). Others define it as the estimated model coefficient associated with the SNP values (as in, for example, (4) and (18)). However, both the accuracy and the interpretability of these approaches depend on the ability of the underlying model to describe eQTL action. This issue is a primary component of this paper.

Careful consideration of an appropriate model for eQTL action also has the potential to affect detection accuracy, since in general p-values under a mis-specified model will be inaccurate. So far, however, the intuition that strong eQTLs will be declared significant under most reasonable models has allowed other concerns to take precedence. For instance, the need to control Type-I error has motivated rank-based transformations for gene expression, even though (as we argue in this paper) such transformations destroy relevant information about the true relationship of the eQTL. Furthermore, most approaches to eQTL analysis are restricted to models that may be fit by ordinary least-squares, which currently is the only computationally viable option for trans-eQTL (full-genome) studies (10).

In this paper we propose an eQTL model which is motivated first and foremost by the biological underpinnings of eQTL action. This model involves an additive effect of allele count and multiplicative component random noise, two features which we argue are well-supported by observed data and biological intuition. Throughout we refer to

the model with the acronym “ACME” (Additive-Contribution, Multiplicative-Error). After a logarithmic transformation, the ACME model is readily represented as a non-linear regression model. We derive an associated iterative least-squares fitting algorithm, and have software for large-scale eQTL analyses that is computationally comparable to available packages for existing models. However, due to the biological importance of ACME’s linearity in allele count on the original scale of gene expression, we refer to the model informally as being “log-of-linear” in nature.

The organization of the rest of this paper is as follows. In the remainder of this section, we expound on some existing approaches to eQTL modeling, and describe in more detail the statistical setting of eQTL analyses. In Section 2, we motivate and lay out the ACME model in detail, and conduct statistical tests on real data to show its ability to well-characterize eQTL action. In Section 3 we perform an in-depth analysis of the robustness of ACME model p-values to potential violations of model assumptions in real data. In Section 4 we provide a small example of a downstream real data analysis which is made interpretable by use of the ACME model. In Section 5 we provide a summary of our analysis and results, and discuss future research directions.

1.1 Existing approaches to gene expression modeling

In general, there are multiple ways to approach the analysis of gene expression data. First, we point out that gene expression is almost never handled on its original scale, due to heteroskedasticity and heavy-tailed errors (17). Many approaches to expression modeling, especially in cancer studies, are based on binomial, negative-binomial, or poisson generalized linear models (13, 26, 27). However, these types of models are almost never used in eQTL analyses due to relatively long computation time for the associated fitting procedures.

Instead, for eQTL studies, two approaches are dominant. First, a standard linear regression model is often used in conjunction with a log-transformation of expression values (e.g. (15)). This approach is also taken in cancer studies (e.g. (16), (11)). Ultimately, count-based and log-based approaches to gene expression are closely related, due to the binomial GLM log-link function. The second common handling of gene expression in the eQTL setting is the inverse quantile-normalization transformation (e.g. (5)), applied to ensure Normality of residuals under the null (3, 20).

Each of these approaches to gene expression have drawbacks as candidates for application to eQTL effect size analyses. First, quantile-normalization is inherently rank-based, and thus when used in a regression setting can yield nearly identical p-values for very different signal-to-noise ratios (see Appendix A.4). Furthermore, rank-based regression coefficients have no relationship to the original scale of the

data, and are therefore not interpretable in terms of a particular concept of allelic effect. These characteristics make the quantile-normalization approach inappropriate for eQTL effect size analysis.

In contrast, the \log_2 -transformation implies an exponential allelic effect. For instance, the estimated SNP coefficient from \log_2 regression on eQTL data is the estimated fold-change in expression due to the presence of an additional minor allele. However, little has been done to verify that the fold-change interpretation is natural, either biologically or statistically, to the eQTL setting. Is it reasonable to assume allele presence contributes exponentially to gene expression? Questions like these the central focus of Section 2 of this paper.

1.2 Framework and notation

The statistical setting of this paper is within a general framework for eQTL studies, in which n samples attain both genotype and gene read count data from a given experiment. The gene read count data can be stored as a $T \times n$ matrix (where $T > 0$ is the number of transcript sites), having general row vector c of length n giving the number of reads per sample. We scale the columns of this matrix according to a method described in Appendix A.1. Similarly, the genotype data can be stored as a $S \times n$ matrix (where $S > 0$ is the number of genomic loci), having general row vector s of length n giving minor allele count per sample. These genotype values may be imputed, though for the purposes of this paper we make a rounding adjustment described in Appendix A.1. The n samples involved in the study may also have p covariates (like gender or batch) which can be stored as a $p \times n$ matrix.

Throughout this paper, real data analyses will be performed only on “cis” gene-SNP pairs, which are those pairs for which the gene transcription start or end site is within 1 mega-base pairs of the SNP location. “Trans” gene-SNP pairs are all other pairs outside this window. Though we have not replicated the model validation results from this paper on trans-pairs, we find no *a priori* reason to suppose they would be drastically different. We expect that, in general, the ACME model may be applied without regard to genome distance between gene and SNP.

2 The ACME model and diagnostics

In this section we motivate the ACME model through a short list of simpler models that are in some way problematic for the purpose of effect size estimation. First, as remarked in Section 1.1, the assumption that normal residuals are additive on the original scale of expression data is unreasonable. This rules out, for instance, linear

regression models on the original scale of the data. To further support this idea, in Appendix A.3 we give an analysis which compares normality statistics of residual vectors from the standard linear regression model to those from models involving a multiplicative noise term (which assume normality of additive errors on the log-scale). We find that both the normality and homoskedasticity assumptions are violated more commonly with the former model.

Of course, we still see many violations of normality under multiplicative error models. (For comparison, the plots in Appendix A.3 also show results on residuals from the quantile-normalized linear model, which is nearly perfectly normal.) We consider this to be somewhat unavoidable, since a proper effect-size model should include expression data on some “natural” scale which will be inherently noisy and non-normal. The effort, then, should be in finding a scale of expression data for which errors are empirically normal *enough* to be robust to systematic errors in estimation and inference. In Section 3, we show that the log-scale of expression data is appropriate in this sense. Thus, whatever the systematic component of the model, we assume the error component is additive and normal after a log transformation of gene expression.

2.1 Log-based models

What remains to be considered, then, is the true systematic form of allelic effect on log-expression. The focus of this section is the modeling of eQTL action for a single gene-SNP pair (though the full analysis setting involves independent estimation for millions of pairs). Therefore, following notation from Section 1.2, let $y_i := \log(1 + c_i)$ denote the log-transformed normalized gene read count from sample $i \leq n$. As is common practice with log transformations of gene expression, we add 1 to preserve zeros in the data. Let s_i denote the minor allele count for the SNP of sample i ($s_i = 0$ for genotype AA , $s_i = 1$ for genotype Aa or aA , and $s_i = 2$ for genotype aa). Define ϵ_i as $\text{Normal}(\mu = 0, \sigma > 0)$ error for sample i , independently and identically distributed to other samples. Finally, let \mathbf{Z}_i denote the $p \times 1$ vector of covariates for the sample i , and γ an unknown $p \times 1$ covariate coefficient¹.

In the context of log-based eQTL models, the least restrictive modeling assumption is that the mean of y_i has arbitrary, non-functional dependence on s_i . In other words, each genotype yields a different mean of log-expression, and these means are in general

¹Here, σ and γ are each unique to the gene-SNP pair under study, but may differ across pairs. Also, it is common practice in eQTL studies to assume that the covariate effect $\mathbf{Z}_i^T \gamma$ contributes to expression on the same scale as additive, normal noise. We follow this practice for all models considered in this paper (including linear regressions with both raw and quantile-normalized gene expression).

unrelated. This yields what we call the “log-ANCOVA” model, written

$$y_i = \alpha_0 \mathbb{1}_0(s_i) + \alpha_1 \mathbb{1}_1(s_i) + \alpha_2 \mathbb{1}_2(s_i) + \mathbf{Z}^T \gamma + \epsilon_i, \quad (2.1.1)$$

where the α_j parameters are unknown log-expression means corresponding to the genotypes, and $\mathbb{1}_j(s_i) = 1$ indicates that $s_i = j$.

However, there are biological reasons to suppose that gene expression depends functionally on allele count, in a fixed direction. The simplest log-based model incorporating this assumption is linear regression of log expression on genotype and covariates, which was used in previous work mentioned in Section 1.1. We call this the “log-linear” model, written

$$y_i = \theta_0 + \theta_1 s_i + \mathbf{Z}_i^T \gamma + \epsilon_i, \quad (2.1.2)$$

where θ_0 is the unknown “baseline” mean of log-expression, and θ_1 is the unknown linear contribution to log-expression of each minor allele. Use of this model is, effectively, to suppose that the effect of each additional minor allele on the *original* scale of expression is exponential. In other words, θ_1 is the “fold change” induced by additional minor alleles. This model is the basis of the existing “log-transformation” approaches mentioned in Section 1.1.

2.2 The ACME Model

However, the fold-change interpretation given by the log-linear model may not be biologically natural to eQTL action. We conjecture that, instead, additional minor alleles contribute *additively* to gene expression on its original scale, instead of exponentially. Therefore, we propose the following log-based non-linear regression model:

$$y_i = \log(\beta_0 + \beta_1 s_i) + \mathbf{Z}_i^T \gamma + \epsilon_i. \quad (2.2.1)$$

Above, β_0 is the unknown “baseline” mean of *raw* expression, with β_1 the unknown linear contribution of s_i . This linearity on the original scale of expression is made apparent by exponentiating of both sides of Equation 2.2.1²:

$$c_i + 1 = (\beta_0 + \beta_1 s_i) \times (\exp\{\mathbf{Z}_i^T \gamma\}) \times \exp\{\epsilon_i\}. \quad (2.2.2)$$

The above equation represents the ACME model in its most primitive form, since it makes clear the model’s asymmetry between the noise component, which is multiplicative, and the systematic component, which is additive. However, Equation (2.2.1) is a more natural representation for statistical fitting and inference, since it includes additive normal errors. To fit the ACME model, we use a Gauss-Newton-style algorithm, derived in Appendix B.

²Note that in Equation (2.2.1), $\exp\{\epsilon_i\}$ has the log-Normal distribution with mean 1, so the expectation of c_i is completely determined by the systematic part of the model.

The natural effect size

We argue that it makes the most sense, from a biological perspective, to define β_1/β_0 as the “natural” eQTL effect size of interest. This is to interpret the effect size in “units” of the baseline expression β_0 . It is often of interest to consider how much each minor allele “brings” the expression above or below baseline. In Section 4 we provide a basic exploratory data analysis with the ACME model which illuminates this issue.

The effect size β_1/β_0 also has a mathematically elegant interpretation in terms of a particular representation of the ACME model. Note that the log-based formulation of ACME (Equation (2.2.1)) may be written

$$y_i = \log(\beta_0) + \log\left(1 + \frac{\beta_1}{\beta_0}s_i\right) + \mathbf{Z}_i^T\gamma + \epsilon_i. \quad (2.2.3)$$

The above formulation separates the role of β_0 in determining baseline expression and the role of β_1/β_0 in determining the SNP effect. Equation (2.2.3) is also particularly useful in the derivation of the fitting algorithm in Appendix B. For the rest of this paper, we take “effect size” to mean the β_1/β_0 parameter from this representation of ACME.

2.3 Model fit diagnostics

In this section we compare the exponential and linear assumptions for eQTL allelic effect by performing goodness-of-fit tests for the log-linear and ACME models. We sub-sampled a large eQTL data set from the GTEx Project (12). The scheme to sub-sample the data was based on intuition that model diagnostics for mis-specified models should be more revealing when signal from the true model is stronger. Since strong eQTLs are the minority, we set up a sampling scheme to over-sample strong eQTLs, based on a preliminary measure of strength. We describe this more fully in Appendix A.2.

Goodness-of-fit test statistic

As the log-linear and ACME models are each “nested” within log-ANCOVA, the log-ANCOVA model may be expressed in terms of their parameters. As a consequence, if either model is sufficient to explain variation in gene expression, the log-ANCOVA fit will be statistically indistinguishable from the fit of that model. For instance, if the true model is log-linear, then the log-ANCOVA mean estimates will fall roughly on the line given by the log-linear model.

This of course does not suggest that using log-ANCOVA is a sufficient approach regardless of whether a smaller model fits equally well. All else being equal, we should prefer parsimonious models. In particular, both log-linear and ACME are quantitative in allele count alone, whereas log-ANCOVA is categorical in genotype. So, the discovery that either model fits as well as log-ANCOVA would be grounds to investigate biological understandings of eQTL action in terms of allele count. Furthermore, a smaller model allows more degrees of freedom, which yields more statistical power.

The F statistic relating sums of squares residuals is natural to test the null assumption that a nested model is sufficient for a particular data set. Define SSR_1 as the sum of squared residuals from the fit of log-ANCOVA, and SSR_0 as the sum of squared residuals from the fit of any nested model. Then the test statistic in our setting is $F = \frac{SSR_1 - SSR_0}{SSR_1 / (n - p - 3)}$ which is F -distributed with 1 and $n - p - 3$ degrees of freedom³. A p-value for the test is then obtained from the upper-tail CDF for this F distribution.

Results

For both the log-linear and ACME models, we applied this test to every gene-SNP pair in the sub-sampled data. Figure 1 shows that the distribution of F p-values from log-linear tests grow increasingly non-uniform as eQTLs become stronger. As mentioned at the start of this section, this strongly suggests the log-linear model is a mis-specification, and that a fold-change interpretation of allelic effect may not be natural for most eQTLs.

In contrast, p-values for the ACME model are approximately uniform for eQTLs of all strengths, implying that fits from the ACME model are, on the whole, statistically indistinguishable from those of log-ANOVA. As mentioned at the outset of this section, this implies the ACME model is, overall, sufficient to describe eQTL action. We emphasize that these results imply no other eQTL model with two parameters which is substantially different from ACME will be sufficient in this sense. All such models will display deviation from the log-ANOVA for stronger eQTLs, as we saw with the log-linear model.

Remark: We replicated the results in Figure 1 by applying the same sub-sampling and testing pipeline to eight other GTEx data sets (corresponding to tissues other than Thyroid). We display some of these in Appendix D.

³This statistic is asymptotically F -distributed when it involves non-linear models fit via maximum likelihood.

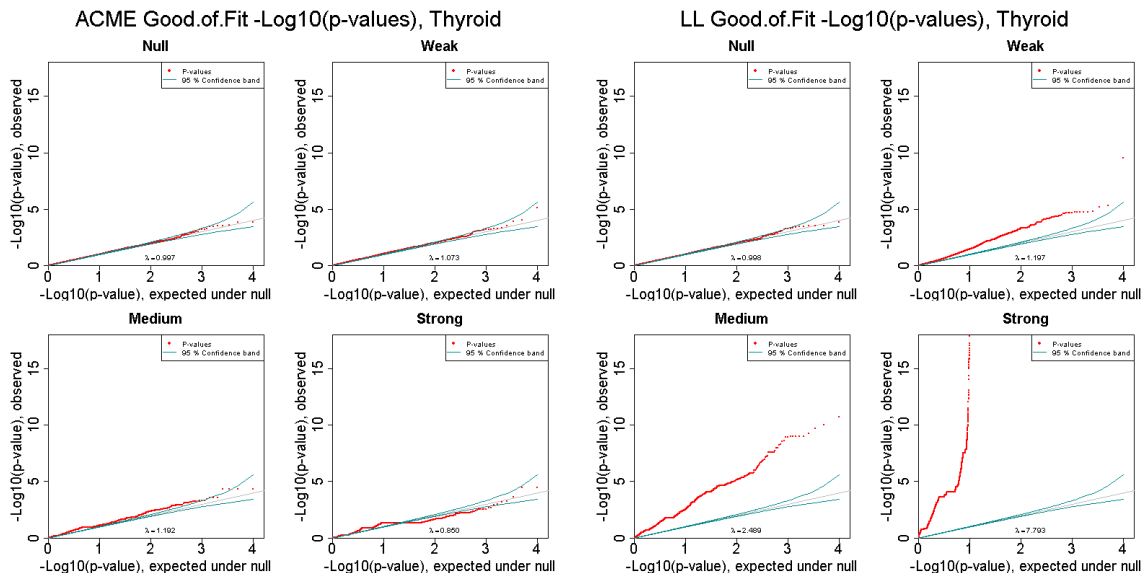


Figure 1: Q-Q plots of likelihood ratio test p-values for ACME and LL models, in each sector of sample data. The grey line is where we would expect the p-values (represented by the red dots) to fall if they were perfectly uniform, and the green line represents the 95% window of error around this expectation. λ is the inflation factor.

3 Model p-values and Type I error

In this section we address in more detail the assumption of residual normality, first mentioned in Section 2. Violations of this assumption are most concerning in their effect on Type I error, which is a central issue in genomic studies. In particular, the large number of tests performed in eQTL analyses presents a special challenge for false positive control. For cis-analysis, the number of tests is typically on the order of 10^7 (12), while for trans-analysis, the number of tests can exceed 10^{10} . Using a Bonferroni bound for control of family-wise error at 0.05 requires p -values accurate to the order of $\alpha = 10^{-9}$ for cis-analysis and to $\alpha = 10^{-12}$ for trans-analysis.

This issue can be spoken of in terms of p-value distributions: given a hypothesis test and choice of test statistic, it is ideal to somehow ensure that p-values are uniformly distributed under the null. As mentioned in Section in 1.1, this can be achieved in the eQTL setting by using p-values from a linear regression model with quantile-normalized gene expression data. However, while these p-values are correlated with those derived from the ACME model, they are different enough to produce a substantially different set of rejected eQTLs. Those eQTLs at the threshold of statistical significance are especially affected. Therefore, we propose instead to use

a p-value derived from the F -statistic directly associated with the ACME model. Explicitly, for each gene-SNP pair, we are interested in the hypotheses

$$H_0 : \frac{\beta_1}{\beta_0} = 0 \quad \text{vs.} \quad H_a : \frac{\beta_1}{\beta_0} \neq 0$$

After fitting the ACME model and a reduced mean-model with $\beta_1 = 0$, we compute the F -statistic associated with these hypotheses (which is similar to that from Section 2.3, but with $n - p - 2$ secondary degrees of freedom).

We wish to determine if, on a real eQTL data set, we can expect the above test to produce uniform p-values under the null. In general, there are two potential causes of non-uniformity. The first is that additive residuals for log-transformed gene expression may be too non-normal. As mentioned in Section 2, our results in Appendix A.3 show that residual vectors from log-based eQTL models sometimes do not pass the Wilks-Shapiro test for normality. Second, since ACME is a non-linear regression model, the F test is only asymptotically exact. In the following sections we aim to show that neither of these potential sources of error are problematic in practice.

3.1 Empirical performance of the F test

Our first method to investigate the empirical performance of the F test is to simulate 1 million highly realistic null gene-SNP pair data sets. In particular, the true residual vector used to construct each pair was a residual vector from the preliminary data, estimated with the ACME model. Our complete simulation method is described in Appendix C.1. We fit both the ACME and log-linear models to the full set of simulated gene-SNP data and computed the associated F -statistic p-value for each. The results are shown in Figure 2.

Note that the F -test appears exact for the log-linear fit. This implies that any non-normality inherent to the data from the GTEx project (when expression is log-transformed) negligibly affects the performance of the F -test. The distribution of log-linear model p-values effectively isolates the first potential source of pvalue non-uniformity described at the outset of this section. The second source of potential non-uniformity (the non-exactness of the F test under non-linear maximum likelihood methods) may be isolated by comparing the ACME p-value distribution to the log-linear distribution. The deviation is noticeable only for the few lowest p-values. Overall, the inflation factors show that the distributions are indistinguishable. These observations are initial support for the robustness of the proposed F test.

Remark: We have also explored the application of an existing method for precisely conservative permutation p-values under the null. This method is known as

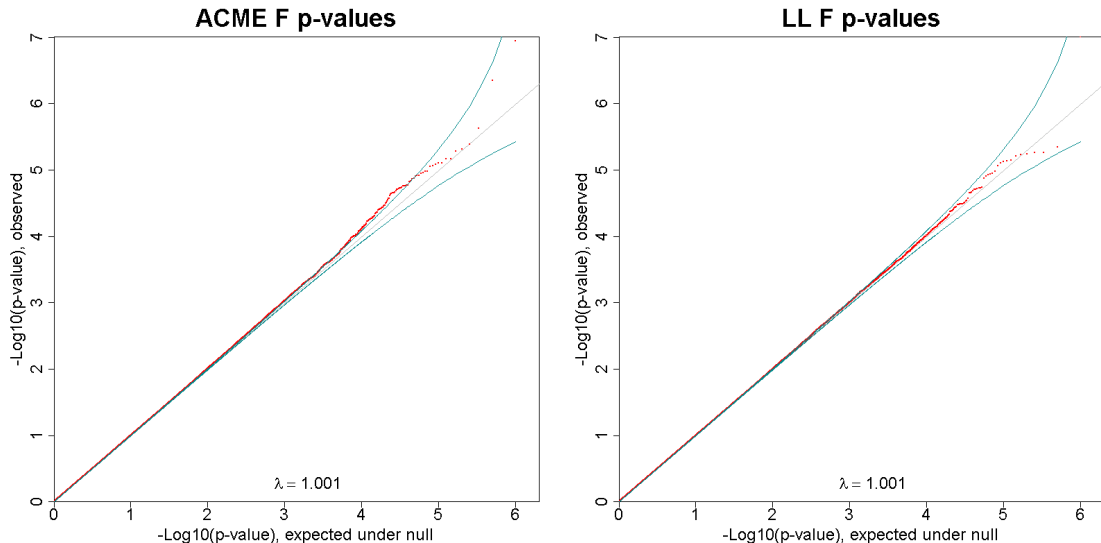


Figure 2: p-value distributions from null simulated data with realistic errors and real covariate/genotype data. λ values are inflation factors.

Moment Corrected Correlation (MCC), introduced in (25). We briefly describe the method and its application in Appendix C.2.

3.2 Estimation of Type I error with importance sampling

The analysis in the previous section was an initial, direct approach to assess accuracy of the p -values from ACME model F -statistics. However, 1 million simulated pairs is insufficient to assess the far tail of the p -value distribution. We are unaware of any attempts via direct data simulation to quantify robustness in eQTL studies to the stringent levels described at the outset of this section, e.g. in situations in which we can expect some true-null p -values below 10^{-9} . For example, the robustness investigations of (17) likewise used only 10^6 simulations for each simulation condition.

A computationally efficient way to assess Type-I error rates for massive amounts of tests is to perform importance sampling (21), in which samples are drawn from an appropriate alternative distribution (with $\beta_1 \neq 0$), and then re-weighted to provide an estimated null rejection probability. For regression models, the skewness in the error distribution can affect false positive control (25). Accordingly, we used the skew-normal model (2) for the distribution of errors ϵ , with skewness determined by a parameter δ . The model elucidates the effect of skew on false positive control, with $\delta = 0$ corresponding to the assumed normal error model. Simulations were performed

for the relatively modest average expression $\beta_0 = 100$, with error variance of $\sigma^2 = 1$, modest minor allele frequency 0.1, and for sample sizes $n = 100, 250$ and 500. As the vast majority of gene-SNP pairs in the GTEx dataset used in this paper showed skewness values in ACME residuals between -0.5 and 0.5 (see Appendix C.3, Figure C10 for an example using Adipose GTEx pilot data), we chose the skew-normal parameter to roughly correspond to this skewness range (details in Appendix C.3). Target type I error values α ranged from 10^{-20} to 10^{-1} .

The results for the ACME F -test p -values are shown in Appendix Figure C10, using the importance sampling approach as detailed in Appendix C.3. Some general conclusions can be made. For $n = 100$ and negative skewness in ϵ (with $\delta = -0.45$), the ACME p -values are noticeably conservative for $\alpha < 10^{-6}$. For positive skewness, the p -values are slightly anti-conservative, but comparatively more accurate than for negative skewness, due to asymmetry in the behavior of the systematic component of the ACME model. For larger $n = 250$, the conservativeness under negative skewness is less extreme, and p -values reasonably accurate to $\alpha = 10^{-9}$ for the skewness range shown. We conclude that p -values for the ACME model produce sufficient Type-I error rates for cis-eQTL analysis for $n = 250$ or greater, and can be somewhat conservative. For trans-analysis, larger sample sizes may be required. However, (24) suggested that sample sizes of > 1000 are necessary to reliably detect trans-eQTLs, which would presumably provide further robustness in the p -values.

4 Effect size and average expression

Though it is not the primary purpose of this paper is to provide novel real data analyses, in this section we provide a basic application of the ACME model. In particular, this example lacks interpretability without confidence in the reliability of effect size estimates, which we argue ACME provides. As representative data sets, we chose 10,000 cis-eQTLs uniformly at random from various tissue-specific data sets from the GTEx project, and produced ACME estimates for each pair. Figure 3 shows a basic scatter plot of the estimated effect sizes from Thyroid against the average normalized read count for each corresponding gene. The figure shows that as baseline expression increases, the magnitude of effect size goes down. This suggests that in eQTL action, it is difficult for alleles to cause practical changes in gene expression when the gene is already highly expressed. Results from more GTEx tissues are given in Appendix D.

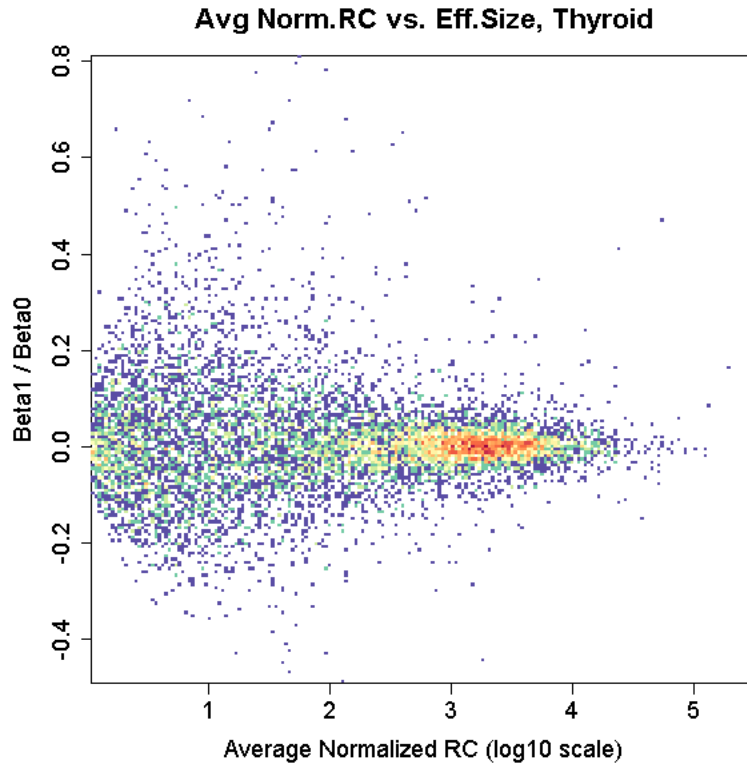


Figure 3: Additional effect-size/average normalized read count comparisons

5 Discussion

In this paper we proposed and defended ACME, a new eQTL model for individual gene-SNP pairs. The motivation for ACME is based on a careful analysis of real eQTL data and a reasonable biological conception of eQTL action. Our analyses revealed that existing approaches to eQTL analysis, while useful for some purposes, do not account for the precise functional relationship between allele count and gene expression. Using real data, we showed that the systematic component of the ACME model is the best-fitting description of eQTL action among two-parameter models involving allele count. Thus, fitting the ACME model yields reliable eQTL effect sizes that have a ready biological interpretation.

We also showed that the F -test corresponding to the effect size of the ACME model is robust to the magnitude of model assumption deviations seen in real data. Due to this, and the demonstrated ability of ACME to capture the functional form of eQTL action, this implies that p-values from the ACME model will be more accurate

than those from existing eQTL models. Efforts are underway to compile a publicly available software package for the fast fitting of the ACME model on tens of millions of gene-SNP pairs. Once this is completed, the authors recommend incorporating ACME p-values into eQTL analyses in which p-values and effect sizes of individual gene-SNP pairs are relevant.

Future research directions will involve extending the ACME model to multiple SNPs, or to multiple gene expression vectors (a multiple-regression extension). More importantly, however, much future research in which reliable, interpretable eQTL effect sizes are relevant is now available on a large-scale. A major motivation of our work was the opportunity to provide a solid foundation from which to make inferences about estimated eQTL effect sizes, and their relationship to other phenotypic data. With this paper’s introduction of the ACME model, we believe this is now possible.

5.1 Acknowledgements

The GTEx data used for the analyses described in this article were from dbGaP accession number phs000424.v3.p1 (<http://www.gtexportal.org>). The GTEx Project was supported by the Common Fund of the Office of the Director of the National Institutes of Health (commonfund.nih.gov/GTEx). The work of various authors on this paper was supported in part by NIH R01MH101819-01, NSF DMS1310002, EPA R835802, and NHGRI HG007840. The research and analyses in this paper were spurred along by many helpful conversations and phone calls with members and working groups from the GTEx Consortium.

Appendix A

A.1 Particulars of data preparation

A few specific adjustments were made to the basic data framework described in Section 1.2:

1. We round all allele counts from their imputed values (to 0, 1, or 2). Though all models discussed throughout can in principle handle imputed SNP values, rounding them facilitates the goodness-of-fit test described in Section 2.3.
2. To account for the library size of each tissue sample, we standardize each read count matrix as follows. For a fixed tissue, denote the matrix of gene expression readings by the $T \times n$ matrix C . First we compute the entry-wise mean \bar{x}_C of the matrix C . Then we scale each column of C so that it sums to $n^2 T \bar{x}_C$. This

results in a matrix with the same entry-wise sum, but with equivalent library sizes across patients. We assume each gene expression vector c_i has been pulled from this standardized version of C .

A.2 Sampling Scheme for Residual and Goodness-of-Fit Analyses

We created a sub-sampled eQTL data set comprising of equally-sized sets of null, weak, medium, and strong eQTLs. To make these demarcations, we took an *a priori* measure of eQTL strength to be the p-value associated with the quantile-normalized linear regression model⁴ (described in Section 1.1), which were provided with the data set by the GTEx Project. We divided the list of cis-eQTL pairs into four bins: “null” eQTLs with $-\log_{10}$ p-value in $[0, 5)$, “weak” with $-\log_{10}$ p-value in $[5, 10)$, “medium” with $-\log_{10}$ p-value in $[10, 15)$, and “strong” with $-\log_{10}$ p-value in $[15, \infty)$. To finally produce the sub-sampled data, we then sampled 10,000 pairs from each bin, uniformly-at-random.

A.3 Tests of Normality and homoskedasticity

This section contains the results from tests for normality and homoskedasticity of residuals, for each eQTL strength bin, and for all single-pair eQTL models considered in this paper. For each of the 10,000 gene-SNP pairs in each eQTL strength bin (see in Appendix A.2), we calculated the p-value for the canonical Shapiro-Wilk test for normality, and the p-value for the canonical Bartlett test for homoskedasticity. Figure A4 displays boxplots of these p-values on the $-\log_{10}$ scale. We see that residuals for the linear model with raw gene expression (“RAW”) are less Normal and homoskedastic than for the log-based models (ACME, log-linear (“LL”), and log-ANCOVA (“ANCOVA”)). This is particularly true for weak eQTLs for which error assumptions are most important for Type I error control. The green lines represent the typical FDR cut-off applied to each bin of the data. Results from more GTEx tissues are given in Appendix D.

A.4 Quantile-normalized regression vs. ACME regression

An understanding of the information loss brought about by quantile-normalizing gene expression in eQTL analysis can be had by considering two gene-SNP pairs whose

⁴As we suggest in Section 1.1, this measure is imperfect. However, it close enough for our purposes here.

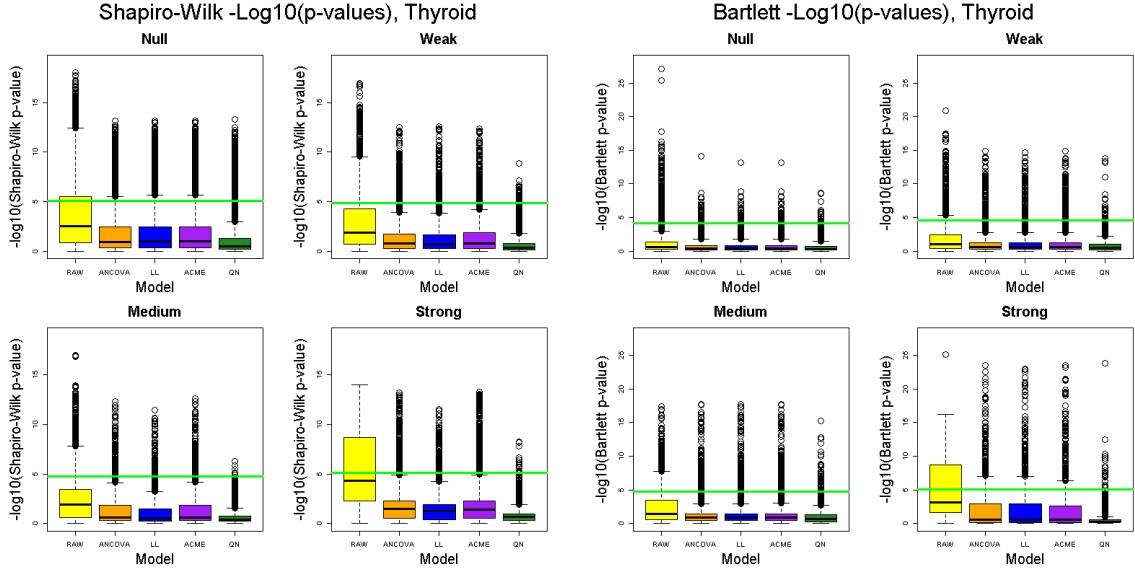


Figure A4: Boxplots of $-\log_{10}$ Shapiro-Wilk and Bartlett p-values from all models

eQTL actions are similar with respect to that transformation, but distinct with respect to a model relating to the natural scale of the data. Countless pairs of eQTLs from the preliminary data set (see Section 2.3 and Appendix A.2) fit this description. We chose one such pair, displayed in Figure A5. While the estimated ACME effect size of pair 2 is ten times greater than that of pair 1, the effect sizes from linear regression with quantile-normalized expression are nearly the same. Furthermore, the baseline expression of pair 1 is far greater than that of pair 2, a distinction also completely erased by quantile-normalization.

Appendix B ACME Fitting Algorithm

Here we give an iterative algorithm used to approximately maximize the likelihood of the ACME model. For a particular gene-SNP pair, this is equivalent to minimizing the sum of squares

$$\sum_i (y_i - \log(\beta_0 + \beta_1 s_i) - \langle \mathbf{Z}_i, \gamma \rangle)^2 \quad (\text{B.0.1})$$

in the parameters $\beta = (\beta_0, \beta_1)$ and γ . The iterative algorithm involves least-squares regression on an approximating linear model. Denoting the natural effect size β_1/β_0 by η , the conditional mean of y_i given \mathbf{Z}_i and s_i has the representation

$$\mathbb{E}[y_i | \mathbf{Z}_i, s_i] = \log(\beta_0) + \log(1 + s_i \eta) + \mathbf{Z}_i^T \gamma \quad (\text{B.0.2})$$

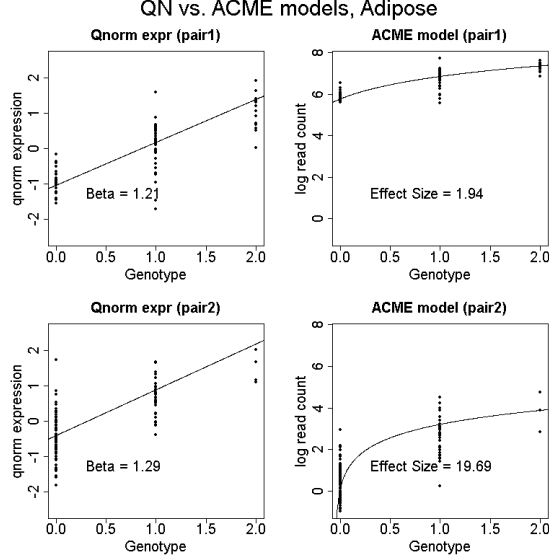


Figure A5: eQTL data from two choice gene-SNP pairs from Adipose tissue. The fitted lines correspond to the estimated parameters from each model.

The first-order Taylor approximation of $\mathbb{E}[y_i | \mathbf{Z}_i, s_i]$ around η at an estimate $\hat{\eta}^j$ is

$$\mathbb{E}[y_i | \mathbf{Z}_i, s_i] \approx \log(\beta_0) + \log(1 + s_i \hat{\eta}^j) + \frac{s_i}{1 + s_i \hat{\eta}^j} (\eta - \hat{\eta}^j) + \mathbf{Z}_i^T \gamma \quad (\text{B.0.3})$$

Letting $\eta_0 := \log(\beta_0)$ and $y^j := y - \log(1 + s_i \hat{\eta}^j)$, subtracting $\log(1 + s_i \hat{\eta}^j)$ from each side of Equation B.0.3 yields the following linear model in $\eta^* := \eta - \hat{\eta}^j$:

$$y_i^j = \eta_0 + \frac{s_i}{1 + s_i \hat{\eta}^j} \eta^* + \mathbf{Z}_i^T \gamma \quad (\text{B.0.4})$$

After fitting this model at the j^{th} iteration, we set $\hat{\eta}^{j+1}$ to $\hat{\eta}^* + \hat{\eta}^j$, and repeat the procedure. This is repeated until $|\hat{\eta}^j - \hat{\eta}^{j+1}|$ is close to machine precision. Then, the final estimates of η_0 and η are used to obtain estimates of β_0 and β_1 via the equations $\hat{\beta}_0 = \exp\{\hat{\eta}_0\}$ and $\hat{\beta}_1 = \hat{\beta}_0 \hat{\eta}$.

Remarks. We set the initial estimate of η to 0. If for any j , $1 + s_i \hat{\eta}^j$ is negative for any index i , we divide $\hat{\eta}^j$ by 2 and restart the j -th iteration.

Appendix C Section 3 Appendices

C.1 Framework for Direct Null Simulation

The preliminary data set used in Section 2.3 contained data from 40,000 unique gene-SNP pairs. When calculating the residual diagnostics presented in that section, we saved the estimated residual vectors (computed by the ACME fit) from each gene-SNP pair. We used these to create 25 null-data replications of each of the 40,000 pairs from the preliminary data. For a fixed gene-SNP pair, we went through the following steps:

1. Recalled s the real allele count vector, $\hat{\beta}_0$ the ACME-estimated value of β_0 from the preliminary data, and $\hat{\sigma}$ the ACME-estimated value of σ from the preliminary data
2. For $r = 1, \dots, 25$, constructed a vector of realistic errors ϵ_r by

$$\epsilon_r = \hat{\sigma}\epsilon_r^* + \mathcal{N}_r(0, \hat{\sigma}/10)$$

where ϵ_r^* is a randomly selected stored residual vector from one of the 40,000 gene-SNP pairs, scaled to have variance 1. The addition of $\mathcal{N}_r(0, \hat{\sigma}/10)$ is a “jitter” (independent within r and between all 40,000 pairs) to ensure that no two chosen mock-residual vectors are equivalent, while allowing them to retain any inherent non-Normality.

3. Constructed the j -th replication of null gene expression data

$$g_r = \exp \{ \log(\hat{\beta}_0) + Z\gamma_r + \epsilon_r \}$$

where γ_r is $\mathcal{N}_p(0_p, I_p)$ and independent within r and between all 40,000 pairs.

C.2 Moment Corrected Correlation (MCC)

If it is of interest to obtain precisely conservative p-values with ACME model estimates, a relatively fast method for obtaining approximate permutation p-values has been developed by Zhou et. al. in (25). This method is most powerful on linear data, but is conservative in general under the null of no association (linear or otherwise). The MCC approximation is based on higher moments of correlation under random permutation of the observed data.

We show two sets of figures to portray the usefulness of MCC. For four different tissues, and on 10,000 randomly chosen cis eQTLs within each tissue, we calculated MCC p-values, direct (random) permutation p-values, and linear regression p-values. In each case, the p-value corresponds to the association between

$\log(1 + \text{normalized read counts})$ and allele counts⁵. In Figure C6, we show compare MCC p-values to those obtained from permutation. We see a very close fit, with deviation in the tails due to resolution loss for low permutation p-values. In Figure C7, we compare the log-linear regression p-values to those same permutation p-values. We see much more spread here, which verifies the success of MCC in matching the direct-permutation p-values.

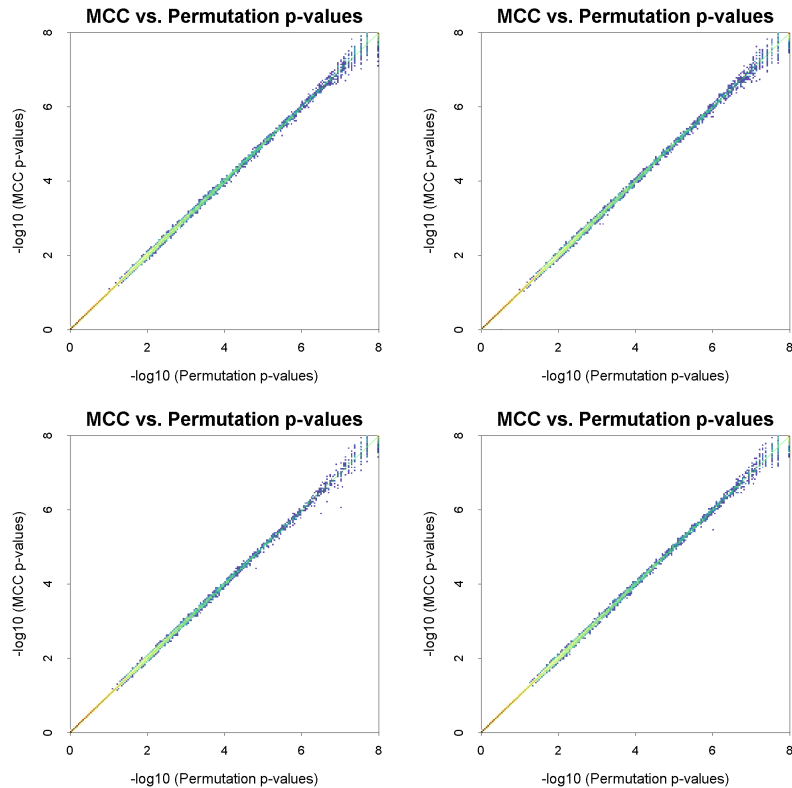


Figure C6: MCC p-values vs. real permutation p-values, each method applied to log-transformed normalized read count vs. rounded allele counts (from Adipose, Artery, Heart, and Muscle, clockwise from the top left).

⁵Though in this paper we argue treating this as a linear association is unjustified, we used this association for convenience. In fact, this gives MCC the opportunity to correct for lack-of-fit.

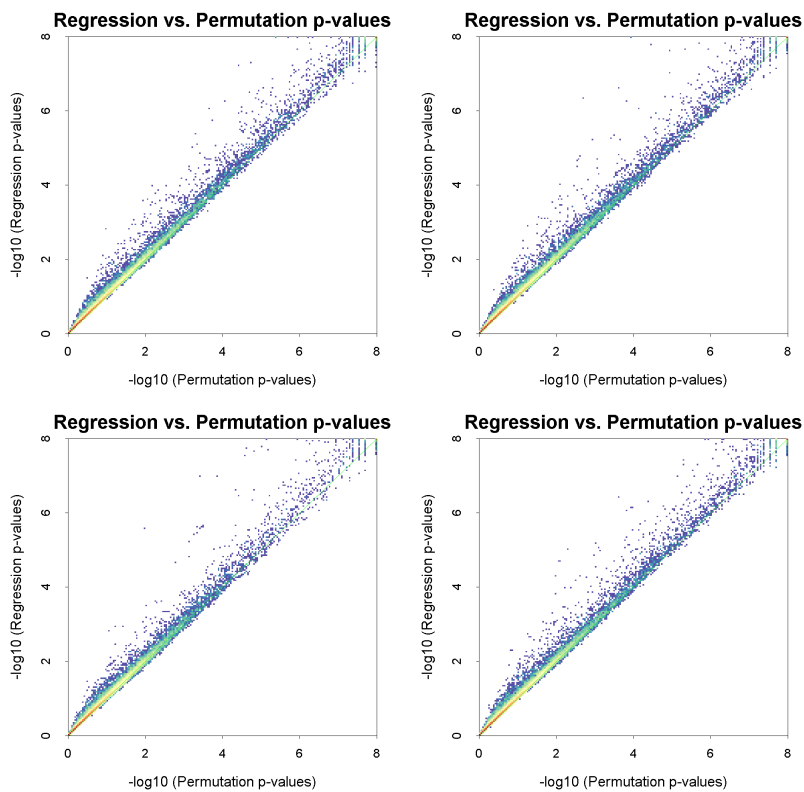


Figure C7: Permutation p-values vs. linear regression p-values, each method applied to log-transformed normalized read count vs. rounded allele counts (from Adipose, Artery, Heart, and Muscle, clockwise from the top left).

C.3 Framework for Importance Sampling

The basic ACME model is

$$y = \log(\beta_0 + \beta_1 x) + \epsilon \quad (1)$$

and $\epsilon \sim N(0, \sigma^2)$. The likelihood ratio and F -statistics both use maximum likelihood estimation of the parameters. For a target type I error α for a single test, we wish to estimate α_{true} , the true probability of rejection under the null. The skew normal density for ϵ provides a simple distribution family to investigate the effect of skew on p -value accuracy. For random variable Z , we have density $g(z) = 2\phi(z)\Phi(\gamma z)$, and define $\delta = \gamma/\sqrt{1 + \gamma^2}$ and $\epsilon = (Z - \xi)/\omega$, where μ and σ^2 are chosen so that $E(\epsilon) = 0$ and $\text{var}(\epsilon) = \sigma^2$. The skewness of ϵ , determined by δ , is $\frac{4-\pi}{2} \frac{(\delta\sqrt{2/\pi})^3}{(1-2\delta^2/\pi)^{3/2}}$.

With importance sampling, it is feasible to estimate α_{true} , even for very small α . Let $F_\eta(x, y)$ be the true joint distribution function for the vectors x and y and f its density, where $\eta = \{\beta_0, \beta_1, \sigma^2, \delta\}$ and σ^2 is the variance of ϵ and δ is its scaled skew parameter. If $\delta = 0$ then ϵ is normal, and if $\delta > 0$ then ϵ is skewed right. Let $p(x, y)$ be the p -value obtained from the F -statistic for x and y . We will use η_0 to refer to the null model $\{\beta_0, 0, \sigma^2, \delta\}$. We have

$$\alpha_{true} = P_{\eta_0}(reject) = \int_x \int_y f_{\eta_0}(x, y) I[p(x, y) < \alpha] dx dy . \quad (2)$$

and I is the indicator function. Simple rejection sampling estimates α_{true} by independently simulating from F_{η_0} K times. For the k th simulation, we compute $a_k = I[p(x_k, y_k) < \alpha]$, and $\hat{\alpha}_{true} = \sum_{k=1}^K a_k / K$. It is easy to show that $\hat{\alpha}_{true}$ is unbiased for α_{true} . However, it is not very accurate unless K is extremely large.

To implement importance sampling for a fixed significance threshold α , we sample data from some alternative distribution F_{η^\dagger} which has the same support as F_{η_0} . When sampling from F_{η^\dagger} , let $b_k = I[p(x_k, y_k) < \alpha] \frac{f_{\eta_0}(x_k, y_k)}{f_{\eta^\dagger}(x_k, y_k)}$. Then

$$E_{\eta^\dagger}(b_k) = \int_x \int_y f_{\eta^\dagger}(x, y) I[p(x, y) < \alpha] \frac{f_{\eta_0}(x, y)}{f_{\eta^\dagger}(x, y)} dx dy = \alpha_{true}, \quad (3)$$

so the importance sampling estimate $\hat{\alpha}_{true}^\dagger = \sum_{k=1}^K b_k / K$ is also unbiased. Through a good choice of η' , $\hat{\alpha}_{true}^\dagger$ can have a much smaller variance than $\hat{\alpha}_{true}$ for a given number of samples K .

Before going further we note that in eQTL applications x corresponds to genotype, and the outer integral in the above equations can be replaced by a sum over possible genotypes. Also, x is assumed to be unaffected by the parameter η in the

eQTL model, so $f_{\eta_0}(x, y)/f_{\eta^\dagger}(x, y) = f_{\eta_0}(y|x)/f_{\eta^\dagger}(y|x)$ and likelihood ratios are also computed conditional on x .

Choosing η^\dagger

To choose η^\dagger , we use the heuristic approach that when sampling from F_{η^\dagger} we wish the F -statistic to reject with probability about 0.5. Determining an appropriate η^\dagger could be done by trial and error, but a faster approach is to use an approximate correspondence between model (1) and linear regression of y on x , with normal errors. Although the difference between a linear model and the ACME model is of key importance for this paper, for the purpose of importance sampling only a crude correspondence needs to hold. We consider the (rare) scenario under the null hypothesis that our linear regression p -value is approximately α . Under such a event, the squared correlation coefficient r_α^2 between x and y can be easily solved, such that the linear regression p -value equals α . Once r_α^2 is obtained, we solve for β_0^\dagger and β_1^\dagger in the true ACME model such that the true correlation between random X and Y is exactly r_α^2 . We also note that even under this rare event that observed x and y appear to be correlated, the mean and variance of the vector y still tends to be near the true values of $\log(\beta_0)$ and σ^2 . Thus, finally, we solve for β_0^\dagger and β_1^\dagger such that

$$E(\log(\beta_0^\dagger + \beta_1^\dagger X)) = \log(\beta_0), \quad \frac{\text{var}(\log(\beta_0^\dagger + \beta_1^\dagger X))}{\sigma^2} = r_\alpha^2. \quad (4)$$

Equations (4) actually provide two solutions, $\{\beta_{0-}^\dagger, \beta_{1-}^\dagger\}$, $\{\beta_{0+}^\dagger, \beta_{1+}^\dagger\}$, according to the sign of r_α , because the form of (1) is not symmetric for positive and negative β_1 . Thus we obtain both solutions and our final importance sampler will sample from each solution with equal probability.

To summarize our approach, using (4) we obtain $\eta_-^\dagger = \{\beta_{0-}^\dagger, \beta_{1-}^\dagger, \sigma^2, \delta\}$, $\eta_+^\dagger = \{\beta_{0+}^\dagger, \beta_{1+}^\dagger, \sigma^2, \delta\}$, and draw importance samples from $F_{\eta^\dagger} = \frac{1}{2}(F_{\eta_-^\dagger} + F_{\eta_+^\dagger})$.

To illustrate our approach to choosing η^\dagger , we performed 10^5 simulations for the null model with skewed errors with $\beta_0 = 100$, $n = 250$, $\sigma^2 = 1$, and skew normal errors with parameter $\delta = 0.97$ (which produces a skewness of 0.78). **Supplementary Figure C9A** shows the p -values as a function of $\hat{\beta}_1$. The red overlay shows the β_1^\dagger values, using each corresponding p -value as the significance level $\alpha/2$ for each tail. The result shows that our approach to selecting β_1^\dagger values appears to be reasonable. **Supplementary Figure C9B** shows the corresponding $\hat{\beta}_0$ values, as well as the β_0^\dagger values. Efficiency of the importance sampler requires that a non-trivial fraction (we target the range of 10%-90%) of the sampled p -values be above and below the target α value. For our setup and $\alpha = 10^{-20}$, we simulated 10,000 datasets from the corresponding F_{η^\dagger} . The distribution of p -values (**Supplementary Figure C9C**) shows that 16% were below α , which is within our target range. **Supplementary Figure**

C9D shows the true rejection probabilities vs the target α values. For this setup, the p -values are highly accurate to $\alpha = 10^{-12}$, but becomes somewhat conservative for smaller α .

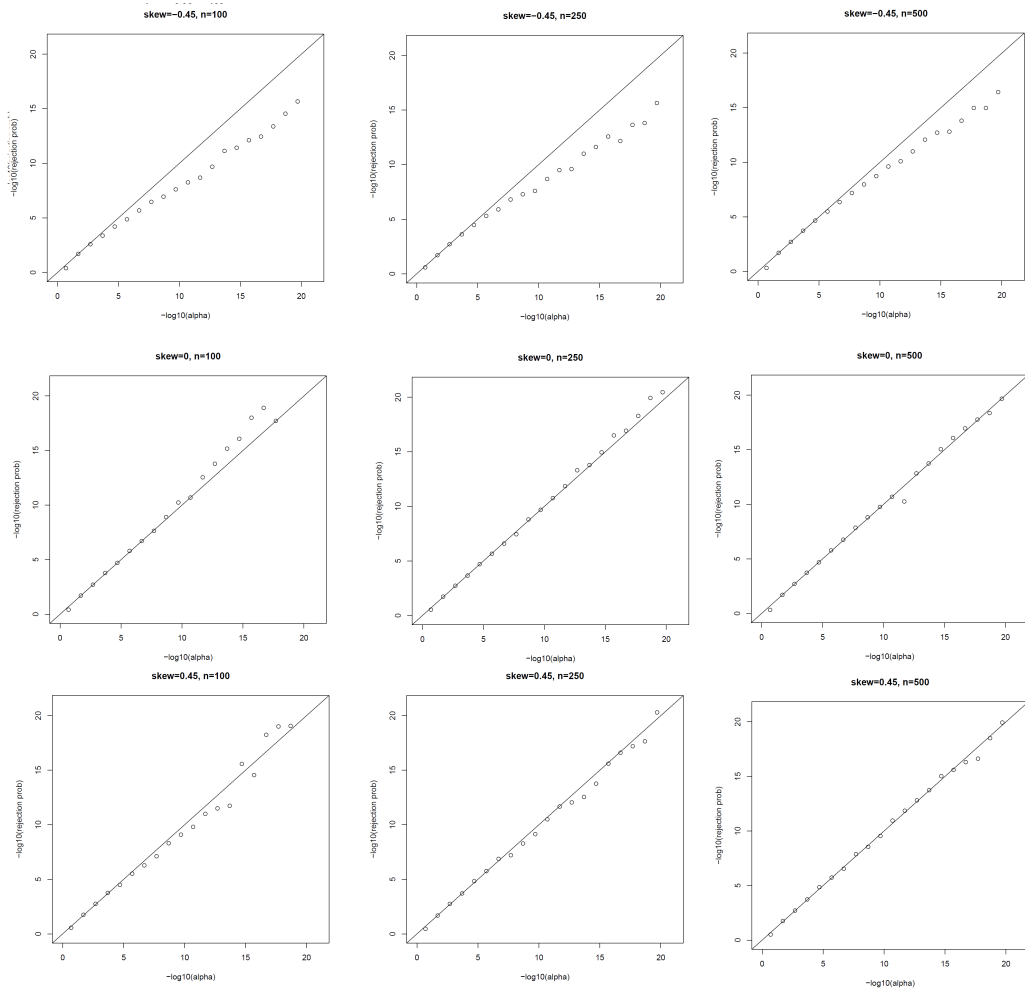


Figure C8: Importance sampling results for ACME F -test p -values (see Section 3.2).

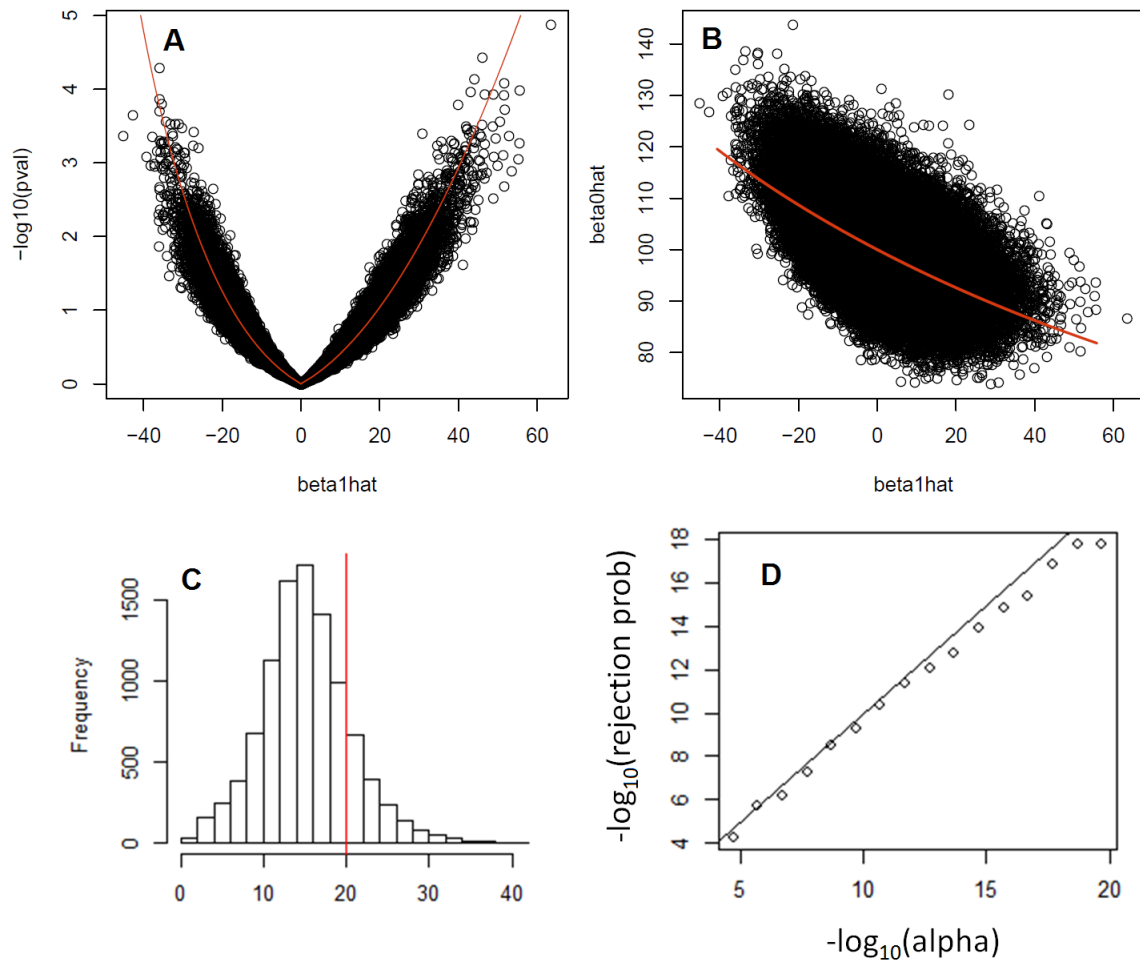


Figure C9: Supplemental figures for Appendix C.3.

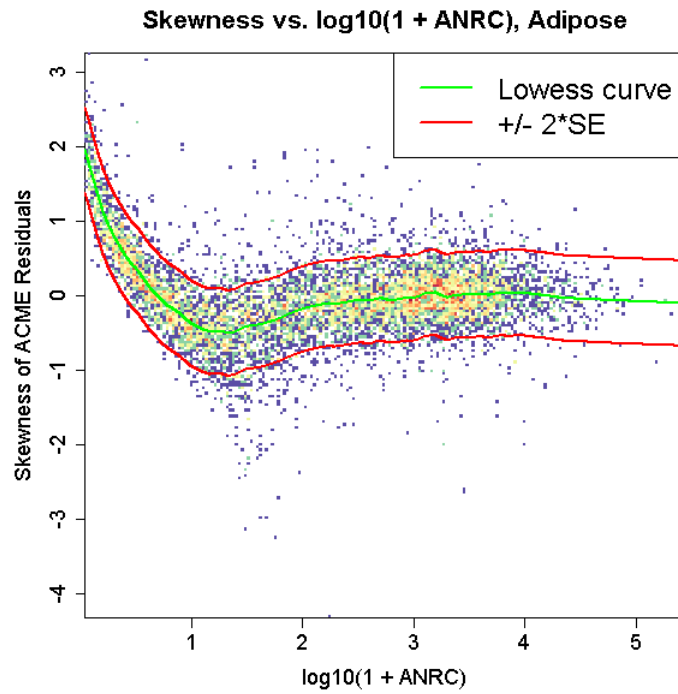


Figure C10: For 10,000 randomly sample gene-SNP pairs from Adipose tissue, the sample skewnesses of eQTL residuals against \log_{10} of the average normalized read counts (across patients) of the gene associated with each eQTL

Appendix D Results from additional GTEx tissues

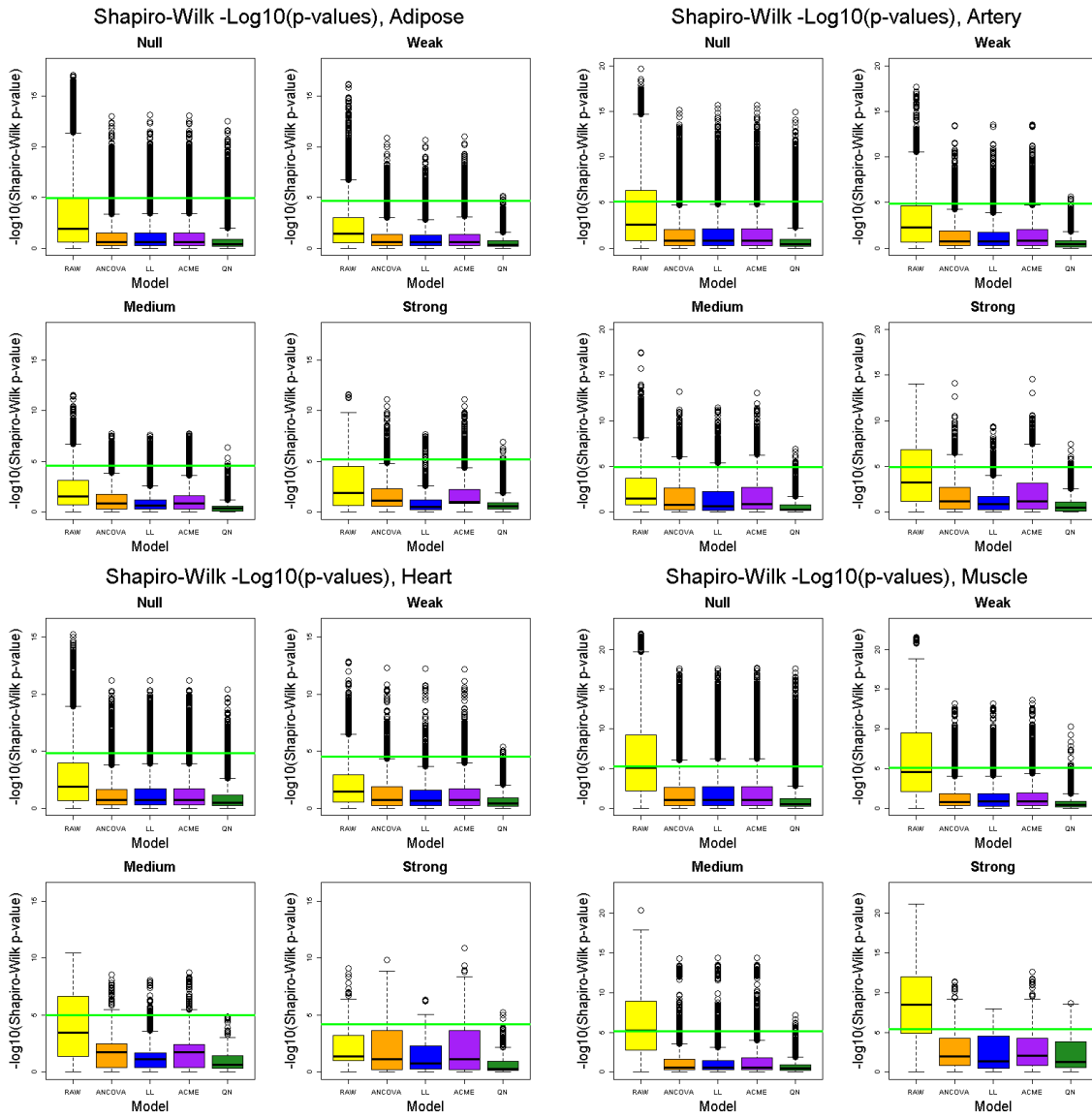


Figure D11: Additional normality test results

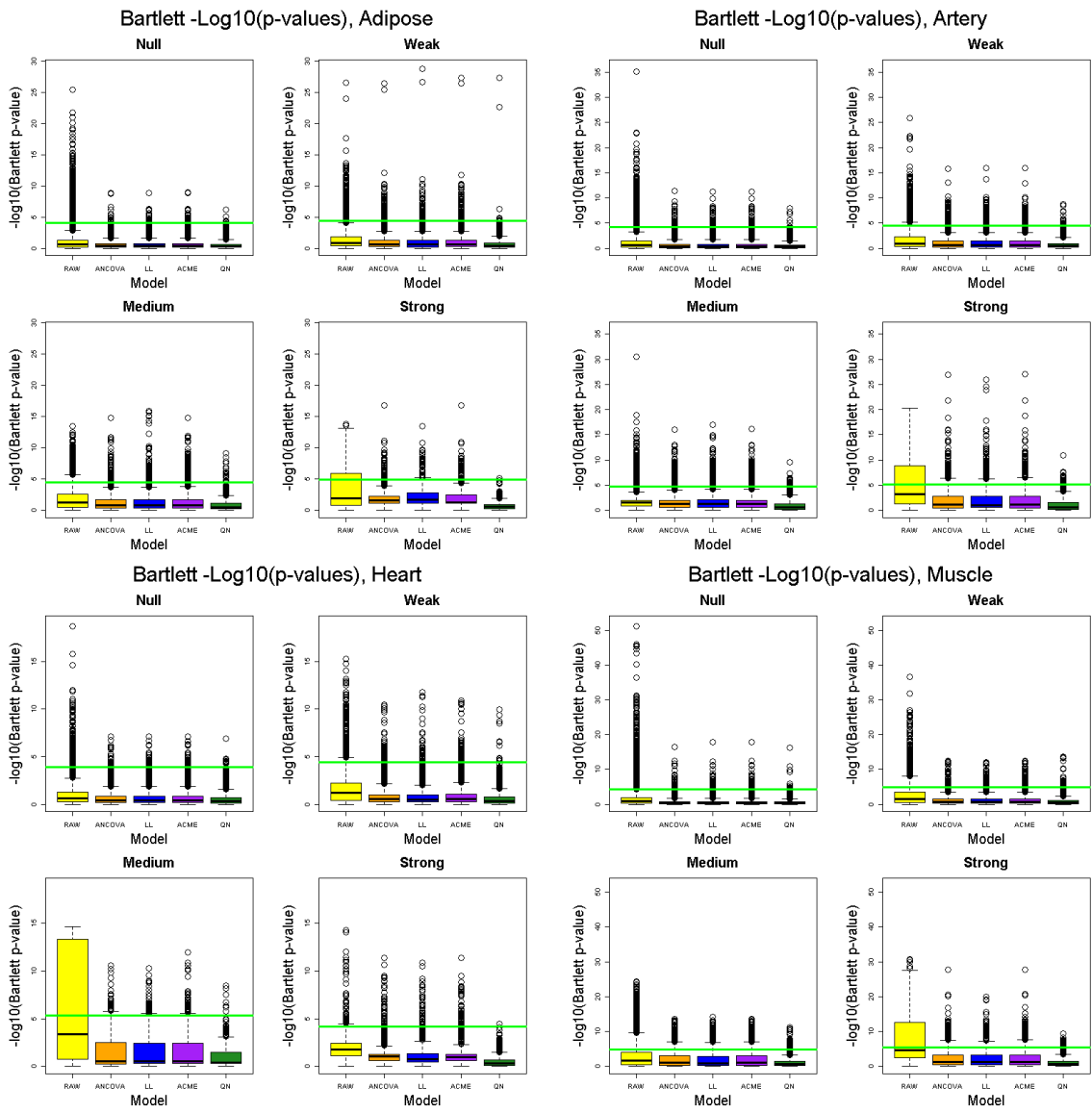


Figure D12: Additional homoskedasticity test results

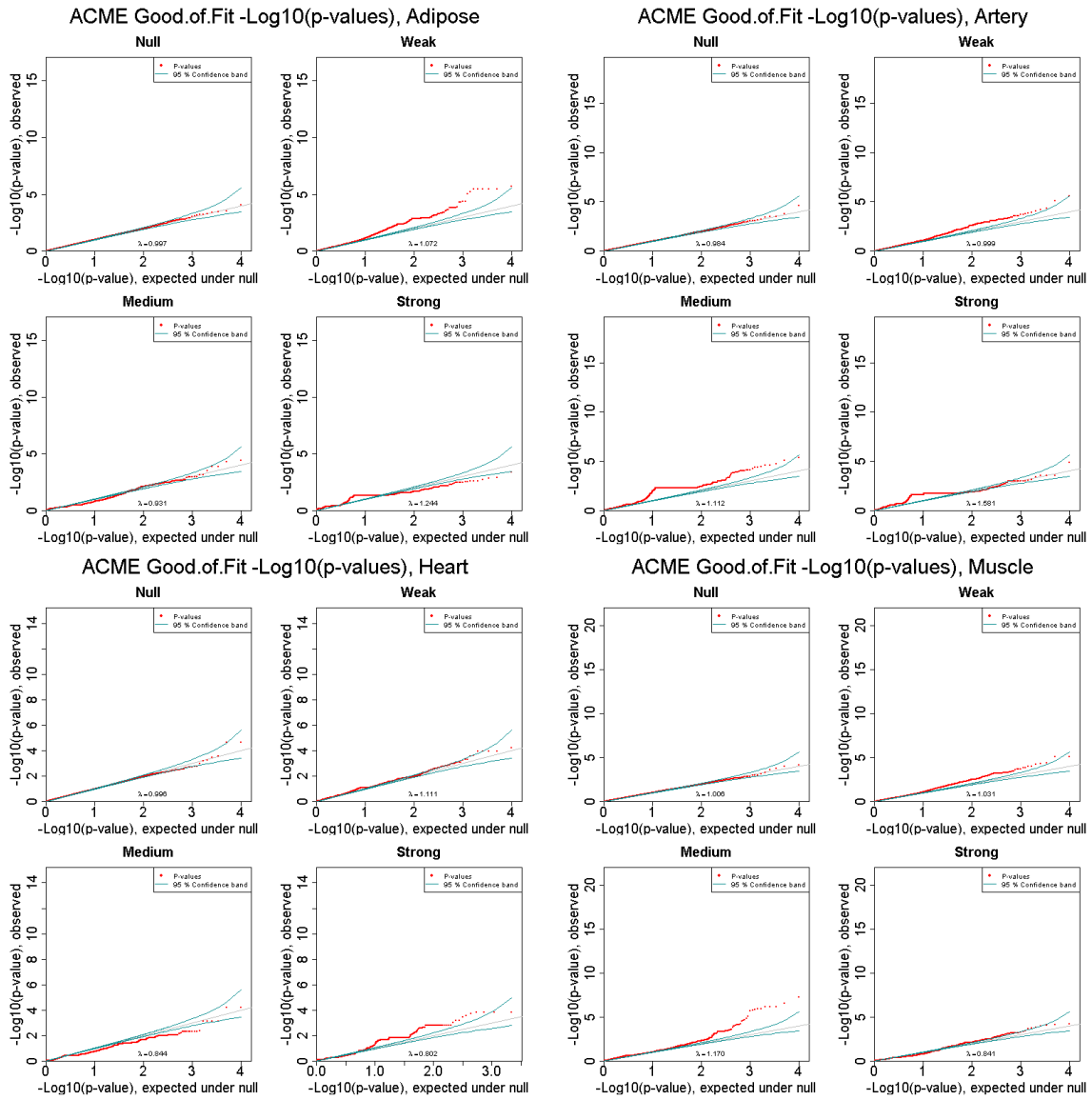


Figure D13: Additional goodness-of-fit test results for ACME

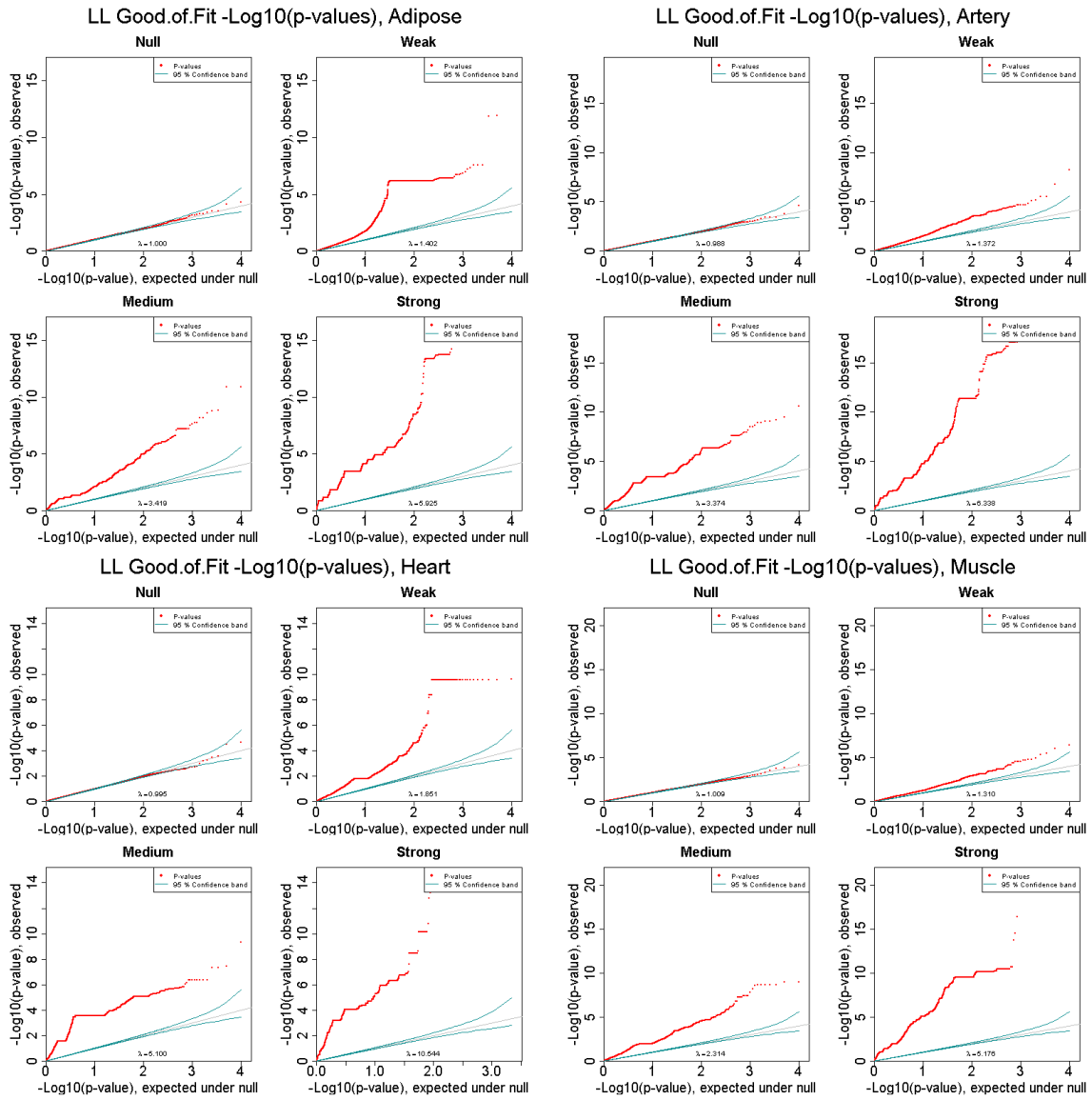


Figure D14: Additional goodness-of-fit test results for log-linear

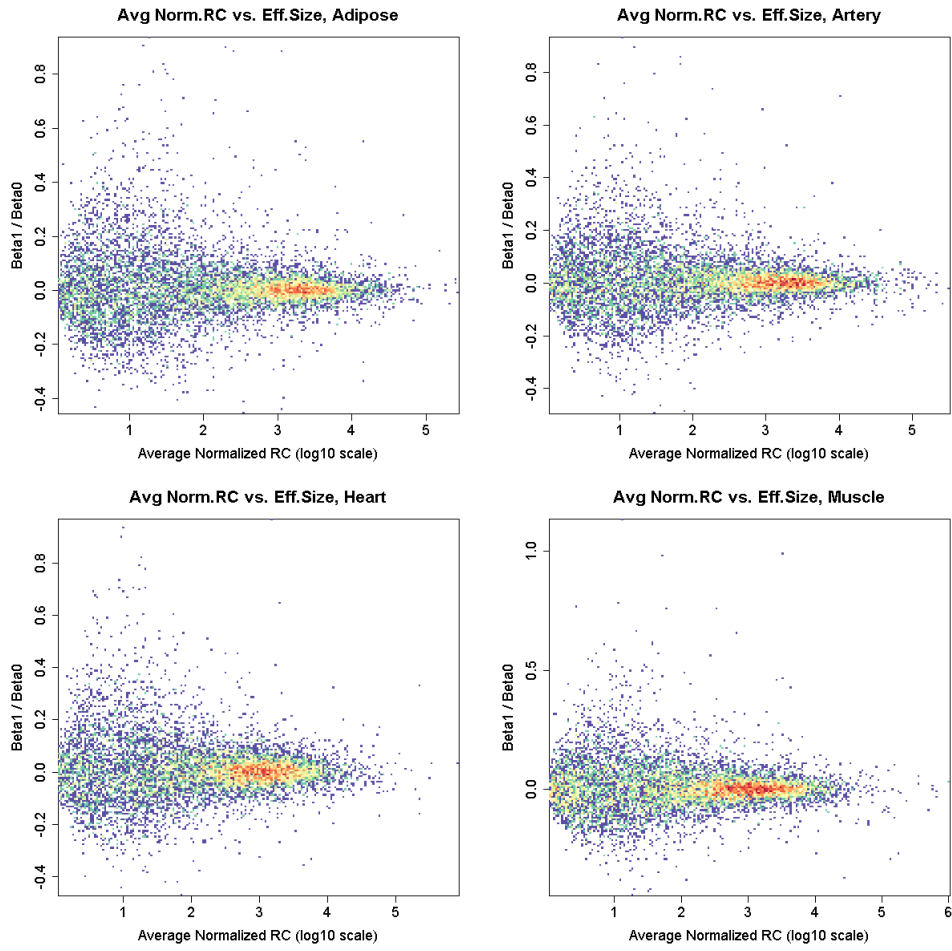


Figure D15: Additional effect-size/average normalized read count comparisons

References

- [1] K. G. Ardlie, D. S. Deluca, A. V. Segrè, T. J. Sullivan, T. R. Young, E. T. Gelfand, C. A. Trowbridge, J. B. Maller, T. Tukiainen, M. Lek, et al. The genotype-tissue expression (gtex) pilot analysis: Multitissue gene regulation in humans. *Science*, 348(6235):648–660, 2015.
- [2] A. Azzalini and A. Dalla Valle. The multivariate skew-normal distribution. *Biometrika*, 83(4):715–726, 1996.
- [3] T. M. Beasley, S. Erickson, and D. B. Allison. Rank-based inverse normal transformations are increasingly used, but are they merited? *Behavior genetics*, 39(5):580–595, 2009.
- [4] J. F. Degner, A. A. Pai, R. Pique-Regi, J.-B. Veyrieras, D. J. Gaffney, J. K. Pickrell, S. De Leon, K. Michelini, N. Lewellen, G. E. Crawford, et al. Dnase [thinsp] i sensitivity qtls are a major determinant of human expression variation. *Nature*, 482(7385):390–394, 2012.
- [5] A. L. Dixon, L. Liang, M. F. Moffatt, W. Chen, S. Heath, K. C. Wong, J. Taylor, E. Burnett, I. Gut, M. Farrall, et al. A genome-wide association study of global gene expression. *Nature genetics*, 39(10):1202–1207, 2007.
- [6] T. Flutre, X. Wen, J. Pritchard, and M. Stephens. A statistical framework for joint eqtl analysis in multiple tissues. *PLoS Genet*, 9(5):e1003486, 2013.
- [7] E. R. Gamazon, H. E. Wheeler, K. P. Shah, S. V. Mozaffari, K. Aquino-Michaels, R. J. Carroll, A. E. Eyler, J. C. Denny, D. L. Nicolae, N. J. Cox, et al. A gene-based association method for mapping traits using reference transcriptome data. *Nature genetics*, 47(9):1091–1098, 2015.
- [8] Y. Gilad, S. A. Rifkin, and J. K. Pritchard. Revealing the architecture of gene regulation: the promise of eqtl studies. *Trends in genetics*, 24(8):408–415, 2008.
- [9] E. Grundberg, K. S. Small, Å. K. Hedman, A. C. Nica, A. Buil, S. Keildson, J. T. Bell, T.-P. Yang, E. Meduri, A. Barrett, et al. Mapping cis-and trans-regulatory effects across multiple tissues in twins. *Nature genetics*, 44(10):1084–1089, 2012.
- [10] Y. Huang, S. Wuchty, M. T. Ferdig, and T. M. Przytycka. Graph theoretical approach to study eqtl: a case study of plasmodium falciparum. *Bioinformatics*, 25(12):i15–i20, 2009.
- [11] Y. Li, M. Liang, and Z. Zhang. Regression analysis of combined gene expression regulation in acute myeloid leukemia. *PLoS Comput Biol*, 10(10):e1003908, 2014.
- [12] J. Lonsdale, J. Thomas, M. Salvatore, R. Phillips, E. Lo, S. Shad, R. Hasz, G. Walters, F. Garcia, N. Young, et al. The genotype-tissue expression (gtex) project. *Nature genetics*, 45(6):580–585, 2013.
- [13] D. J. McCarthy, Y. Chen, and G. K. Smyth. Differential expression analysis of multifactor rna-seq experiments with respect to biological variation. *Nucleic acids research*, page gks042, 2012.

- [14] M. Morley, C. M. Molony, T. M. Weber, J. L. Devlin, K. G. Ewens, R. S. Spielman, and V. G. Cheung. Genetic analysis of genome-wide variation in human gene expression. *Nature*, 430(7001):743–747, 2004.
- [15] A. J. Myers, J. R. Gibbs, J. A. Webster, K. Rohrer, A. Zhao, L. Marlowe, M. Kaleem, D. Leung, L. Bryden, P. Nath, et al. A survey of genetic human cortical gene expression. *Nature genetics*, 39(12):1494–1499, 2007.
- [16] C. G. A. R. Network et al. Genomic and epigenomic landscapes of adult de novo acute myeloid leukemia. *The New England journal of medicine*, 368(22):2059, 2013.
- [17] M. Rantalainen, C. M. Lindgren, and C. C. Holmes. Robust linear models for cis-eqtl analysis. *PloS one*, 10(5):e0127882, 2015.
- [18] A. A. Shabalín. Matrix eqtl: ultra fast eqtl analysis via large matrix operations. *Bioinformatics*, 28(10):1353–1358, 2012.
- [19] B. E. Stranger, A. C. Nica, M. S. Forrest, A. Dimas, C. P. Bird, C. Beazley, C. E. Ingle, M. Dunning, P. Flicek, D. Koller, et al. Population genomics of human gene expression. *Nature genetics*, 39(10):1217–1224, 2007.
- [20] S. Szymczak, M. O. Scheinhardt, T. Zeller, P. S. Wild, S. Blankenberg, and A. Ziegler. Adaptive linear rank tests for eqtl studies. *Statistics in medicine*, 32(3):524–537, 2013.
- [21] S. T. Tokdar and R. E. Kass. Importance sampling: a review. *Wiley Interdisciplinary Reviews: Computational Statistics*, 2(1):54–60, 2010.
- [22] H.-J. Westra, M. J. Peters, T. Esko, H. Yaghootkar, C. Schurmann, J. Kettunen, M. W. Christiansen, B. P. Fairfax, K. Schramm, J. E. Powell, et al. Systematic identification of trans eqtls as putative drivers of known disease associations. *Nature genetics*, 45(10):1238–1243, 2013.
- [23] F. A. Wright, A. A. Shabalín, and I. Rusyn. Computational tools for discovery and interpretation of expression quantitative trait loci. *Pharmacogenomics*, 13(3):343–352, 2012.
- [24] F. A. Wright, P. F. Sullivan, A. I. Brooks, F. Zou, W. Sun, K. Xia, V. Madar, R. Jansen, W. Chung, Y.-H. Zhou, et al. Heritability and genomics of gene expression in peripheral blood. *Nature genetics*, 46(5):430–437, 2014.
- [25] Y.-H. Zhou and F. A. Wright. Hypothesis testing at the extremes: fast and robust association for high-throughput data. *Biostatistics*, page kxv007, 2015.
- [26] Y.-H. Zhou, K. Xia, and F. A. Wright. A powerful and flexible approach to the analysis of rna sequence count data. *Bioinformatics*, 27(19):2672–2678, 2011.
- [27] I. Zwiener, B. Frisch, and H. Binder. Transforming rna-seq data to improve the performance of prognostic gene signatures. *PloS one*, 9(1):e85150, 2014.